magnetochemistry

MDPI

Review

Magneto-Optics Effects: New Trends and Future Prospects for Technological Developments

Conrad Rizal [1,*], Hiromasa Shimizu [2,3] and Jorge Ricardo Mejía-Salazar [4]

[1] Seed NanoTech International Inc., 2 County Crt., Brampton, ON L6W 3W8, Canada
[2] Department of Electrical and Electronic Engineering, Tokyo University of Agriculture and Technology, Koganei, Tokyo 184-8588, Japan
[3] Department of Applied Physics and Chemical Engineering, Tokyo University of Agriculture and Technology, Koganei, Tokyo 184-8588, Japan
[4] National Institute of Telecommunications (Inatel), Santa Rita do Sapucaí 37540-000, MG, Brazil
* Correspondence: conrad.rizal@seed-nanotech.com

Abstract: Magneto-optics (MO) is an effervescent research field, with a wide range of potential industrial applications including sensing, theranostics, pharmaceutics, magnetometry, and spectroscopy, among others. This review discusses the historical development, from the discovery of MO effects up to the most recent application trends. In addition to the consolidated fields of magnetoplasmonic sensing and modulation of optical signals, we describe novel MO materials, phenomena, and applications. We also identified the emerging field of all-dielectric magnetophotonics, which hold promise to overcome dissipation from metallic inclusions in plasmonic nanostructures. Moreover, we identified some challenges, such as the need to merge magneto-chiroptical effects with microfluidics technology, for chiral sensing and enantioseparation of drugs in the pharmaceutical industry. Other potential industrial applications are discussed in light of recent research achievements in the available literature.

Keywords: magneto-optics; magneto-plasmonics; magnetophotonics

check for updates

Citation: Rizal, C.; Shimizu, H.; Mejía-Salazar, J.R. Magneto-Optics Effects: New Trends and Future Prospects for Technological Developments. *Magnetochemistry* **2022**, *8*, 94. https://doi.org/10.3390/magnetochemistry8090094

Academic Editor: Zheng Gai

Received: 15 July 2022
Accepted: 20 August 2022
Published: 24 August 2022

Publisher's Note: MDPI stays neutral with regard to jurisdictional claims in published maps and institutional affiliations.

Copyright: © 2022 by the authors. Licensee MDPI, Basel, Switzerland. This article is an open access article distributed under the terms and conditions of the Creative Commons Attribution (CC BY) license (https://creativecommons.org/licenses/by/4.0/).

1. Introduction

Magneto-optics refers to changes in the properties of light when it is transmitted or reflected in the presence of a magnetic field (externally applied or from a magnetized material medium). These phenomena were first discovered by Michael Faraday in 1845 [1]. He noticed that a linearly polarized light beam undergoes a polarization rotation when it propagates parallel to an externally applied magnetic field. Just over 30 years later, the Reverend John Kerr observed the corresponding effect when he studied the reflection of linearly polarized light from the surface of a magnet [2,3]. These magneto-optics (MO) effects, conventionally called Faraday and Kerr MO effects (in transmission and reflection, respectively), not only helped establish the theory of electromagnetism in the late 19th century, but also laid the foundation for several technological achievements. The Faraday effect, for example, has the unique property of breaking time-reversal symmetry and Lorentz's reciprocity theorem [4], which has been utilized for the development of non-reciprocal optical devices and laser systems [5,6]. The Kerr effect, on the other hand, allows a way to measure or visualize the magnetic state of material media, and has therefore been used for spectroscopy [7–10] and data-storage applications [11–13]. More recently, the advent of nanotechnology and modern nanofabrication tools motivated the exploitation of MO phenomena at micro- and nano-scale levels for a new era of devices, with their optical properties actively manipulated by applied magnetic fields. However, the latter is challenged by weak MO effects at visible and infrared wavelengths [14].

The search for enhanced MO effects at the nanoscale has been led (almost exclusively) by plasmonics over the last few decades, in what is commonly known as magnetoplasmon-

ics [15]. This last approach employs the localized and strongly enhanced plasmonic fields to improve the MO activity of nanostructures [16,17]. Plasmonics refers to the resonant coupling of light with the collective oscillations of the electron cloud (called plasmons) on a metallic surface [18], with the unique ability to concentrate light into deep-subwavelength volumes (enabling devices with unprecedented miniaturization levels) [19]. Magnetoplasmonics has therefore been realized with nanostructures made of pure noble metals [16], pure ferromagnetic metals [20–22], hybrid noble-ferromagnetic metals [23], and hybrid noble metal-ferromagnetic dielectrics [24,25], with applications in (bio)sensing [26–29], nonreciprocal waveguides [30] and magnetic control of the optical chirality [31], among others. Despite these advances, magnetoplasmonic applications are still hampered by the intrinsic losses of metallic inclusions, which has motivated the search for new materials and structures to overcome these challenges. In particular, the reduced level of losses from dielectric ferromagnetic materials [32–35], combined with their integrability with silicon photonics [36,37], has motivated a lot of recent research [38–43]. Moreover, the design and development of hyperbolic MO metamaterials has also gained interest during the last few years [44–48].

In this review paper, we advocate the importance of MO effects for future active nanophotonic devices and their perspectives for industrial applications. The microscopical and macroscopical theory of MO effects (including magnetoplasmonics) have been discussed in several previous works [49–54], to which we refer interested readers. To avoid repetition, we focus our attention here to discuss the most recent trends and future prospects in magnetophotonics, i.e., magneto-optic nanostructures, exemplifying the merging of MO with surface enhanced Raman spectroscopy (SERS), which has already been applied for sensing and magnetic separation of biological moieties.

2. A Brief Review on Magnetoplasmonics

Due to the importance of nanotechnology and magnetophotonics, and also to provide the reader with a historical context, we prefer to start with a brief history of plasmonics. The first experimental evidence of surface plasmon resonance (SPR) phenomenon was observed by Wood in 1902 [55] while measuring the reflectance spectra of a metallic grating. In particular, Wood observed a sharp discontinuous change in the reflectance (around a specific frequency), which was called the Wood's anomaly. Then, in 1907, Rayleight discovered that the frequencies at which anomalies occur are intimately related to the incident angle and wavelength (as well as to the angle of emergence of the diffracted waves), providing a qualitative explanation for the Wood's anomaly [56,57]. However, it was not until 1941 that Fano demonstrated that the physical principle behind the Wood's anomaly stems from the excitation of surface waves at the metallic/dielectric interface [58]. Indeed, Fano indicated the similarity between the Wood's anomaly in the grating and the surface waves in the attenuated total reflection (ATR) effect. Furthermore, in the early 1950s, Pines and Bohm [59–62] showed in a series of papers that conduction electrons in a metal (considered as a free electron gas) can describe collective oscillations, whose quantizations were called plasmons. Based on these previous achievements, Ritchie derived the dispersion relation of SPRs in 1957 [63], which was experimentally demonstrated two years later by Powell and Swan [64]. Merging the ATR analogy (described by Fano) with the SPR dispersion relation, Kretschmann [65] and Otto [66] proposed the use of prism couplers (high-refractive-index incident media) for the excitation of SPRs in flat planar metallic surfaces. On the other hand, the time harmonic oscillation of the electric field component of light forces the density of free charges in metallic nanoparticles to oscillate between upper and lower boundaries. This oscillation exhibits a maximum amplitude at the resonant frequency, analogous to a forced harmonic oscillator [67]. Although in 1904 Maxwell–Garnett used an effective dielectric permittivity theory to explain the colors of glasses containing small metallic nanoparticles [68], the full electromagnetic theory of light scattering and absorption by colloidal metallic nanoparticles was only developed in 1908 by Mie [69]. Plasmonic resonances in metallic nanoparticles are radiative localized (non-

propagating) SPRs (LSPRs), contrary to SPRs in gratings or flat planar metallic surfaces, which are surface-guided modes achieved under phase-matching conditions. These basic plasmonic platforms are illustrated in Figure 1a,b, where the order of electromagnetic decay lengths is also illustrated for each case.

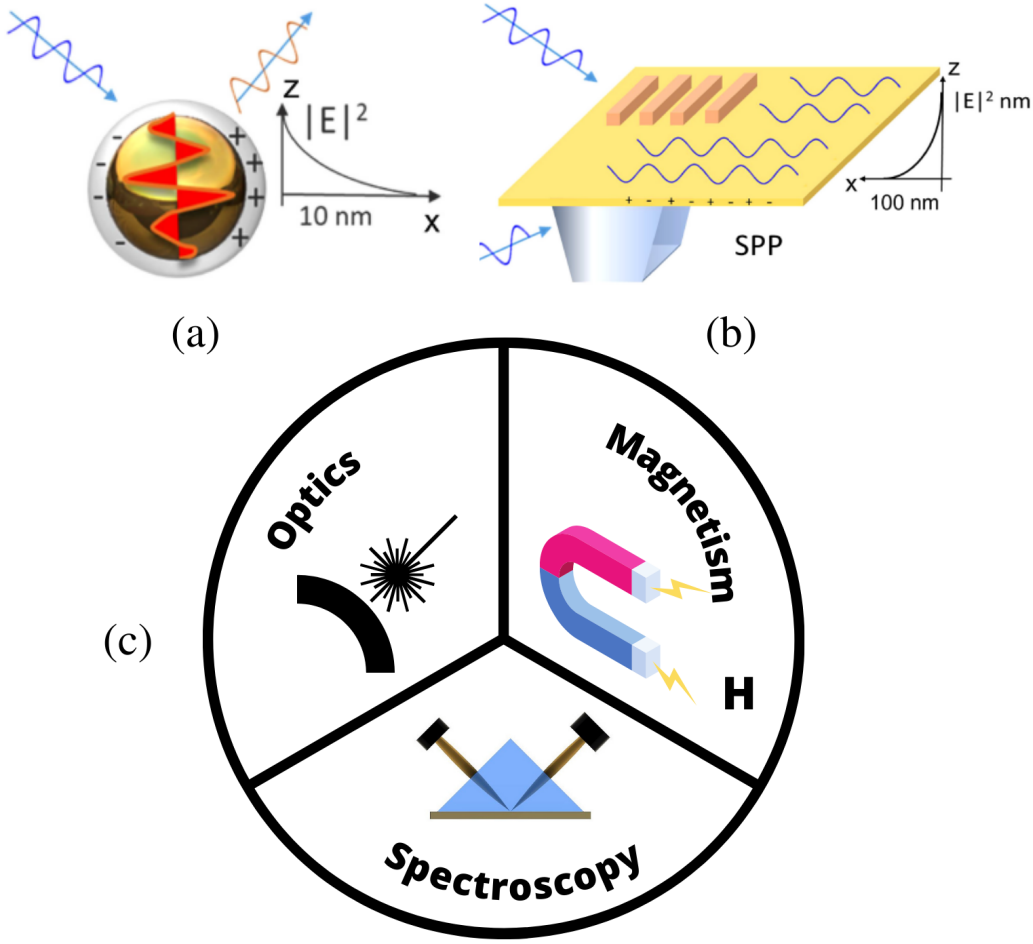

Figure 1. (**a**) Localized surface plasmon resonances (SPRs) and (**b**) propagating SPRs. (**c**) Magneto-plasmonics: merging of optics, magnetism and spectroscopy. Figures (**a**,**b**) were adapted from the American Institute of Physics, 2021 [70]. Copyright 2021 American Institute of Physics.

Since the first experimental demonstrations of SPR applications in gas sensing and biosensing, made four decades ago by Nylander and Liedberg et al. [71,72], there has been intense research activity to enable this technology for the detection of small analytes or in very dilute solutions [73]. However, due to very small changes in the refractive index (RI) of the analyte medium, the resolution of SPR (bio)sensing devices is largely limited by the overlap between nearby resonances. In the search for alternatives to surpass this last drawback, magnetoplasmonic biosensing, i.e., merging plasmonics with magnetism and spectroscopical techniques (illustrated in Figure 1c), has emerged as a promising alternative. The first experimental demonstration of magnetoplasmonic sensing was made by Guo et al. [74], in 1999, who used MO modulation to monitor the phase shift resulting from the minute change of the angle of incidence, demonstrating improved sensing resolutions compared to the conventional SPR approach. Then, in 2006, Sepúlveda et al. [26] demonstrated resolution improvements of up to three orders of magnitude in biosensing applications when using the sharp curves from plasmonically enhanced transverse MO Kerr effect (TMOKE) instead of broad reflectance SPR lines. A prototypical MOSPR experimental setup for sensing is shown in Figure 2a, where a magneto-plasmonic waveguide combining a noble metal (Au in this case) and a ferromagnetic metal (Co in this case) is used in the

Kretschmann-like configuration for improved sensing performance (resolution, sensitivity and detection limit). The MOSPR sensor in Figure 2a is composed by a Au (5 nm)/Co (3 nm)/Au (21 nm) tri-layer film on glass substrate and covered by air (the superstrate). A prism coupler of glass is also used for the ATR mechanism. The reflectance (R) associated with the demagnetized system ($\mathbf{M} = \mathbf{0}$), represented with solid blue circles (see the left axis), is comparatively plotted with the corresponding TMOKE $= \frac{\Delta R}{R} = \frac{R(+M)-R(-M)}{R(+M)+R(-M)}$ values (represented by solid orange circles in relation to the right axis) around a minima of R. From this last result it can be clearly seen that TMOKE curves are sharper than SPR ones, which is used to improve the quality factor and the sensing performance of the structure, as previously mentioned. The superstrate is then successively injected with concentrations of 1%, 2%, 3%, and 4% of ethanol gas diluted with nitrogen, with the corresponding time transient measurements in Figure 2c,d, respectively. As noticed, the signal-to-noise ratio is better for $\Delta R/R$ than that for reflectivity R, showing improved sensitivity by using the MO-SPR sensing. It is worth mentioning that further resolution improvements can be achieved through combined advanced modeling and nanopatterning methods [75–79]. Nevertheless, the MOSPR sensing approach may be inappropriate for detection of very high analyte concentrations, as can be seen in Figure 2d. This last behavior is explained through the close relationship of the optimized TMOKE amplitudes with the SPR phase-matching condition, considering that the latter is lost when the changes in the refractive index are too high.

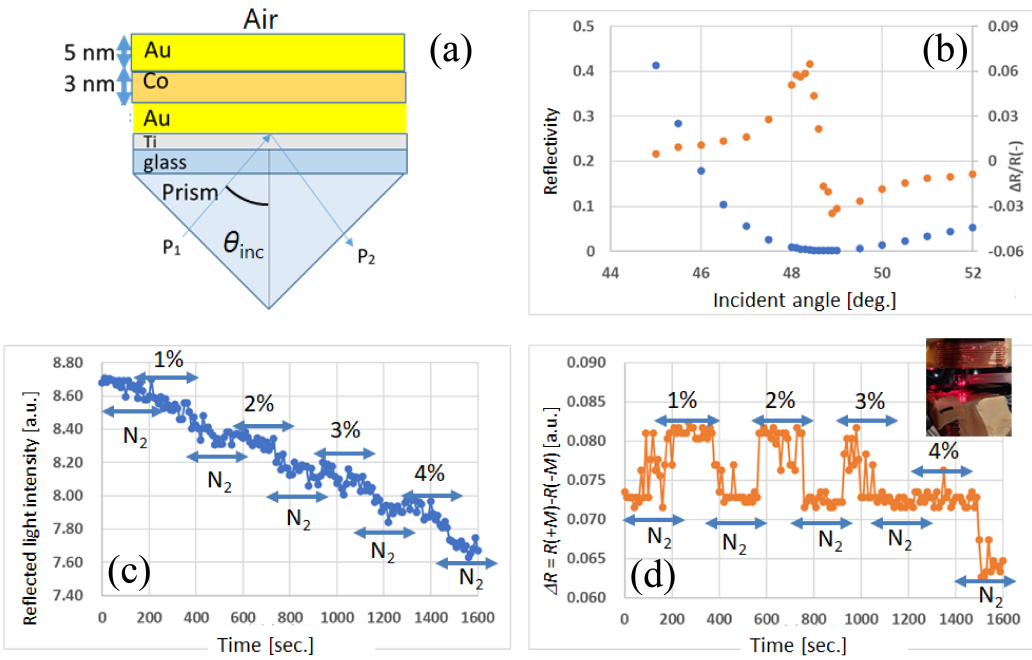

Figure 2. (**a**) A schematic diagram of the fabricated Au/Co/Au MOSPR sensor. A quartz glass prism is mounted on top of the glass substrate, and the light is coupled with an incident angle θ_{inc}. (**b**) The reflectivity measured in air without magnetic field (left axis), and TMOKE $= \Delta R/R$ (right axis). Time transient of (**c**) the reflected light intensity and (**d**) TMOKE upon ethanol gas injection at concentrations of 1, 2, 3, and 4%. In the inset is a photo of the MOSPR sensor chip that was mounted on a quartz prism and positioned between a pair of coils. This chip was part of the Au/Co/Au construction.

Achievements in SPR magnetoplasmonics are not limited to (bio)sensing. For example, the plasmonically enhanced magneto-optic effect is also being actively exploited for new integrated active nanophotonic devices. In particular, high-speed non-reciprocal magnetoplasmonic waveguides have been actively developed during the last years [80–82]. These latter devices enable unidirectional light propagation by actively manipulating the insertion losses for forward and backward modes in a magnetoplasmonic waveguide. This

active tuning is achieved by using an external magnetic field to manipulate the magnetization state of a building ferromagnetic material in the waveguide, as depicted in Figure 3, which in turn alters the insertion loss level in the waveguide. An important application of non-reciprocal waveguides is the stable operation of semiconductor lasers, preventing them from unwanted backward reflection in the optical transmission path. Instead of free space optical isolators consisting of Faraday rotators (magnetic garnet) and two polarizers, semiconductor optical isolators based on the non-reciprocal loss, have been studied, where ferromagnetic metal thin films are deposited at a part of the waveguides. Transversely magnetized ferromagnetic metal provides different propagation loss depending on the magnetization direction or propagation direction, owing to the time-inversion asymmetry. Significantly, on-chip optical isolators can be realized through monolithic integration of semiconductor optical isolators with semiconductor lasers, simplifying the system and avoiding the work of physical alignment between the lasers and isolators [83]. In Figure 4a, we show a cross-section scanning electron microscopy (SEM) micrograph of a semiconductor optical isolator, comprising a ferromagnetic Co thin film on an InP substrate. The vertically magnetized Co thin film provides optical isolation for transverse electric (TE) mode light by using the TMOKE. The experimental setup for optical isolation measurements is shown in Figure 4b, and results showing optical isolation of up to 45 dB/mm are presented in Figure 4c.

The magnetic control of chiroptical activity is a new and fluorishing application of magnetoplasmonics that is increasingly gaining attention [84–89]. The term chirality, used for the first time in 1894 by Lord Kelvin [90], refers to objects that are non-superimposable on their mirror images. Our hands are, perhaps, the most universal example. Because of this analogy, both enantiomorphs (from the Greek's composition enantios = opposite + morphe = form) are conventionally classified as L- (left) and R-enantiomorphs (right) or, when referring to molecules, L- and R-enantiomers. In contrast to achiral (without chirality) environments, where both enantiomers of a chiral molecule (sharing the same stoichiometric molecular formula) exhibit the same physical and chemical properties, molecular chirality plays a key role in the biochemical and biological activity of molecules. In fact, because the elementary building blocks of living organisms (e.g., amino acids and sugars) are chiral, biochemical reactions are inherently chiral [91,92]. The latter is crucially important in pharmacology, where therapeutic effects are associated with a single enantiomer and the other is ineffective or induces serious side effects [93–95], as was demonstrated by the thalidomine disaster in the late 1950s [96–98].

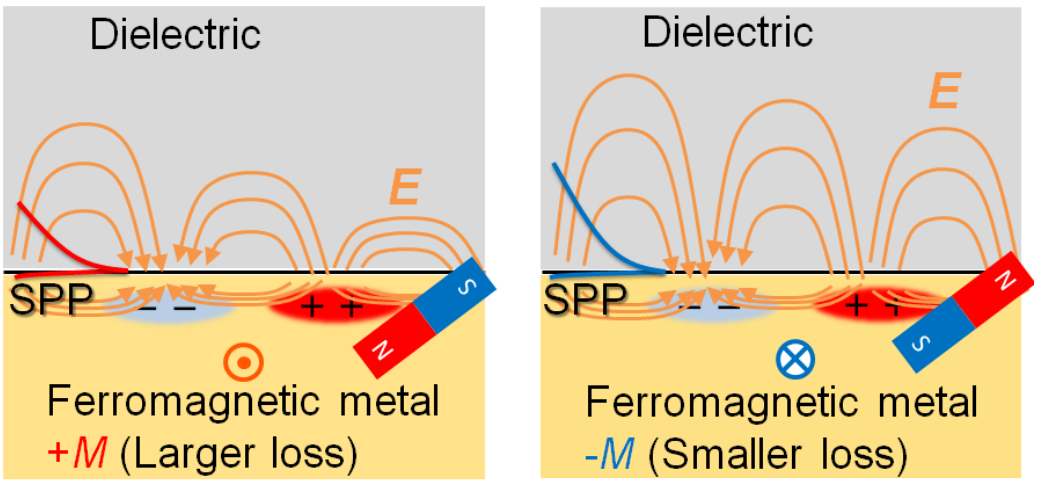

Figure 3. Illustrative representation for the active tuning of insertion losses in a magnetoplasmonic waveguide.

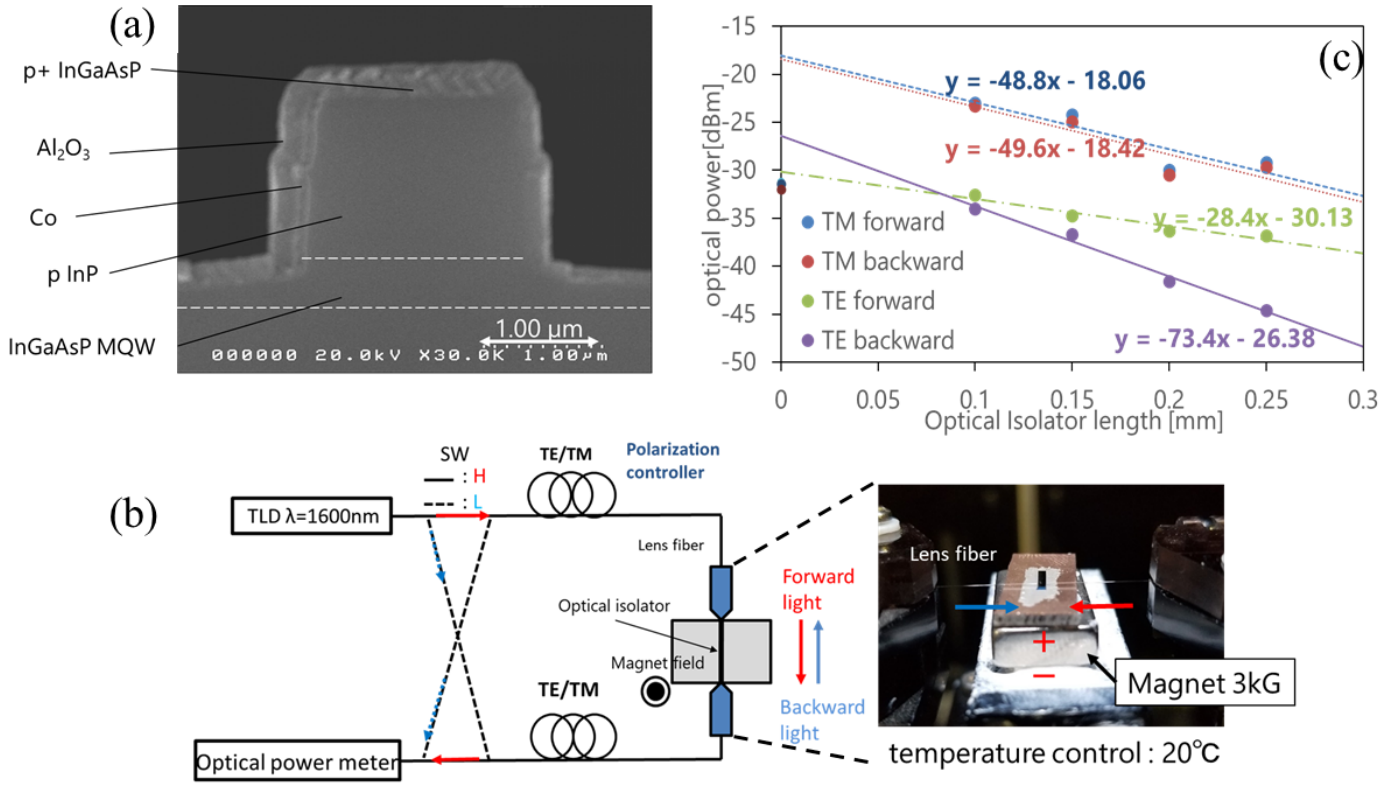

Figure 4. (**a**) A cross-sectional SEM image of the TE mode semiconductor optical isolator. (**b**) A schematic diagram of the experimental setup for measuring the characteristics of semiconductor optical isolators. (**c**) Forward and backward propagation loss as a function of the length of the semiconductor optical isolators.

Although physical and chemical techniques (e.g., circular dichroism and chromatography) are currently used for recognition and separation of enantiomers in the pharmaceutical industry, their performance is still limited to high concentrations or large analyte sizes [99,100]. On the other hand, the Faraday rotation effect is itself chiral. In fact, the physics behind magnetic circular dichroism (MCD), i.e., the differential absorption of left and right circularly polarized light, stems from the Faraday effect [53]. Therefore, through the unique sensing capabilities of plasmonics (using chiral or achiral geometrical designs [101]) with an active CD modulation mechanism [102], the combination of the magnetoplasmonic Faraday effect with circular dichroism (CD) spectroscopy (commonly known as magneto-chiroptical effect) may allow improved detection limits with higher resolutions [103,104]. Figure 5a–c illustrates the magneto-chiroptical application in tuning the extrinsic chiroptical activity from a perforated Au slab, comprising an achiral hexagonal arrange of circular nanoholes [31], whereas Figure 5d,e show the circular differential transmission (CDT) from a chiral arrange of Au and Ni nanoparticles [105]. As was recently indicated in ref. [70], these enhanced magneto-chiroptical effects can be simultaneouly used with magnetoplasmonically enhanced optical forces [106,107] for optical enantioseparation of chiral samples in the pharmaceutical industry.

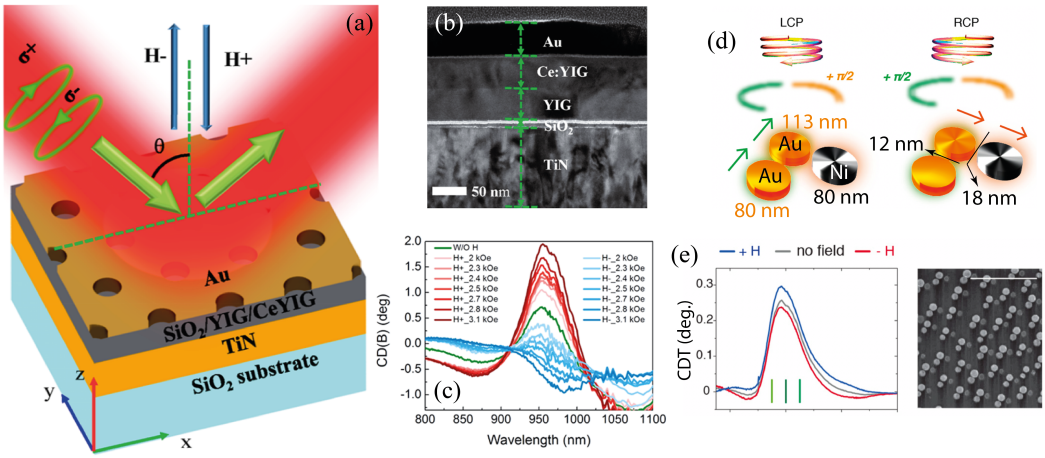

Figure 5. (**a**) Schematic of the magnetoplasmonic multilayer nanostructure for switching the extrinsic optical chirality by using the magneto-chiroptical effect. The applied magnetic field can be alternated between the $+z$ (H+) and $-z$ (H−) directions, as indicated, and the incident CPL can be RCP ($\sigma+$) or LCP ($\sigma-$). (**b**) Different material layer thicknesses are highlighted by using a cross-sectional TEM micrograph. (**c**) Results of magneto-chiroptical effect are comparatively shown with the extrinsic chiroptical activity (without W/O H, see the green line) through CD measurements, for an angle of incidence $\theta = 45°$, by using magnetic field amplitudes varying from −3.1 kOe to +3.1 kOe (applied along the z axis, as illustrated). Reprinted with permission from Qin et al., ACS Nano **14**, 2808 (2020) [31]. Copyright 2020 American Chemical Society. (**d**) Magnetoplasmonic chiral arrange of Au and Ni nanoantennas on a substrate. Green and orange arrows are used to indicate longitudinal resonances of bimetallic nanoparticles, excited with quarter-period phase delay. (**e**) Experimental results for the CDT associated to H+ and H- are comparatively shown with the case without H. Reprinted with permission from Zubritskaya et al., Nano Lett. **18**, 302–307 (2018) [105]. Copyright 2018 American Chemical Society.

3. A Brief Review on All-Dielectric Magnetophotonics

In spite of the tremendous technological achievements using magnetoplasmonic nanostructures, the use of metallic building blocks tacitly implies high absorption losses due to the intrinsic Joule effect. Although researchers have tried to improve the structure and material quality of plasmonic systems [108,109], to reduce losses, energy dissipation remains high and unavoidable. The most recent attempts include the design and development of magnetoplasmonic metamaterials [44–48] that, while demonstrating interesting physical phenomena, are still limited by the use of metallic inclusions. On the other hand, all-dielectric nanostructures exhibiting low optical absorption at visible wavelengths and lossless optical response at the infrared range [110] are gaining interest for modern applications. This interest is mainly fueled by their unique set of optical resonant features, including electric, magnetic and anapole resonances [111–113]. In this context, one of the major drawbacks is the mismatch between the lattice parameters of dielectric MO materials and CMOS compatible semiconductors, which has motivated research on novel materials and manufacturing methods [114–116]. For example, cerium substituted yttrium iron garnet (Ce:YIG) films have been grown on gadolinium gallium garnet substrates, with orientations (100), (110) and (111), through the pulsed laser deposition method [116]. Experimental results for the off-diagonal permittivity component (ε_2) and extinction coefficient (k), shown in Figure 6a,b, demonstrate high MO activity with relatively low optical absorption. These results are of special interest for the development of future non-reciprocal and energy-efficient integrated photonic circuits, with applications in photonic computing and data transport architectures. Indeed, there are currently available several new dielectric MO materials that are monolithically integrable with CMOS technology [36,37,40]. Other recent approaches include the development of transparent MO ceramics [117,118], with applications in Faraday isolators for high-power lasers [119,120].

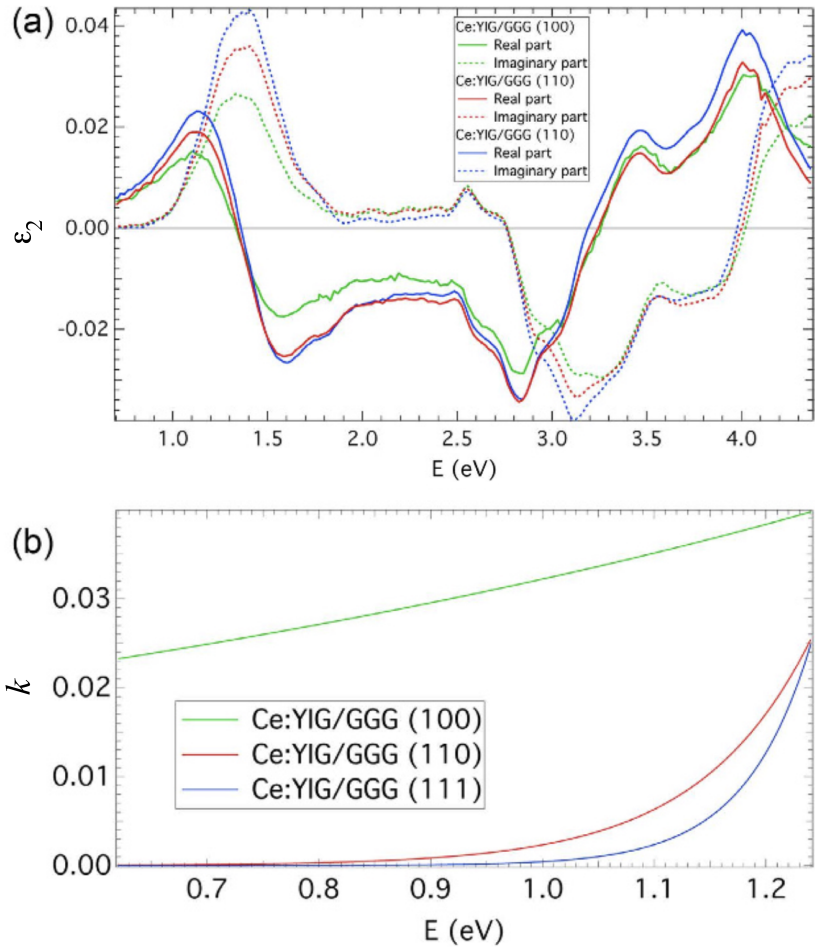

Figure 6. The real and imaginary parts of the off-diagonal permittivity component (ε_2) and the extinction coefficient (k) are shown as a function of the incident wavelength in (**a**,**b**), respectively, for three Ce:YIG samples on GGG substrates. Adapted with permission from ref. [116]. Copyright 2016 Springer Nature.

In addition to new low-loss all-dielectric MO materials, nanostructured all-dielectric MO platforms are also needed to compete with the well-established magnetoplasmonic mechanism for amplified MO effects. Recent achievements include high-Q MO metasurfaces for advanced light control in dual polarizations [33], as schematically represented in Figure 7a. This metasurface consists of a two-dimensional array of Bi-substituted iron-garnet nanopillars, fabricated by electron-beam lithography, on an ultrathin Bi-substituted iron-garnet slab (epitaxially grown on a gadolinium gallium garnet (GGG) substrate). A SEM micrograph of the fabricated structure is shown in Figure 7b. The diffraction properties of the nanopillar lattice enables the coupling between the incident light and the quasi-waveguide modes in the metasurface. Significantly, the nanopillar array exhibits resonances for both TE and TM (transverse magnetic) polarizations, whose field profiles are shown in Figure 8a–d for $TE_{0,1}$ and $TM_{1,0}$, allowing active manipulation of the propagation through changes of the in-plane magnetization (**M**, illustrated in Figure 7a). Other approaches use metal-free MO hyperbolic metamaterials, which can be fabricated with oxide-nitride nanostructures [46]. All these advances have an impact on the photonic integrated circuits (PICs) industry for dynamic optical signal processing at the chip scale [41] and for on-chip MO memories [121]. Applications also include (bio)sensing [122,123], ultrafast optical spin dynamics manipulation [124], and light filtering and modulation [125].

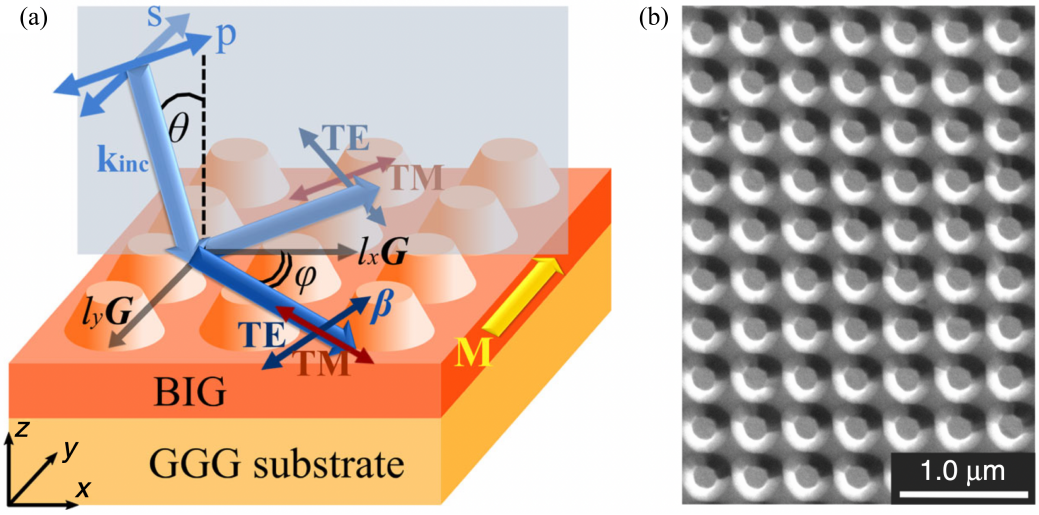

Figure 7. (**a**) Schematic of the metasurface and mode excitation. (**b**) SEM picture of the fabricated microstructure. Adapted with permission from ref. [33]. Copyright 2020 Springer Nature.

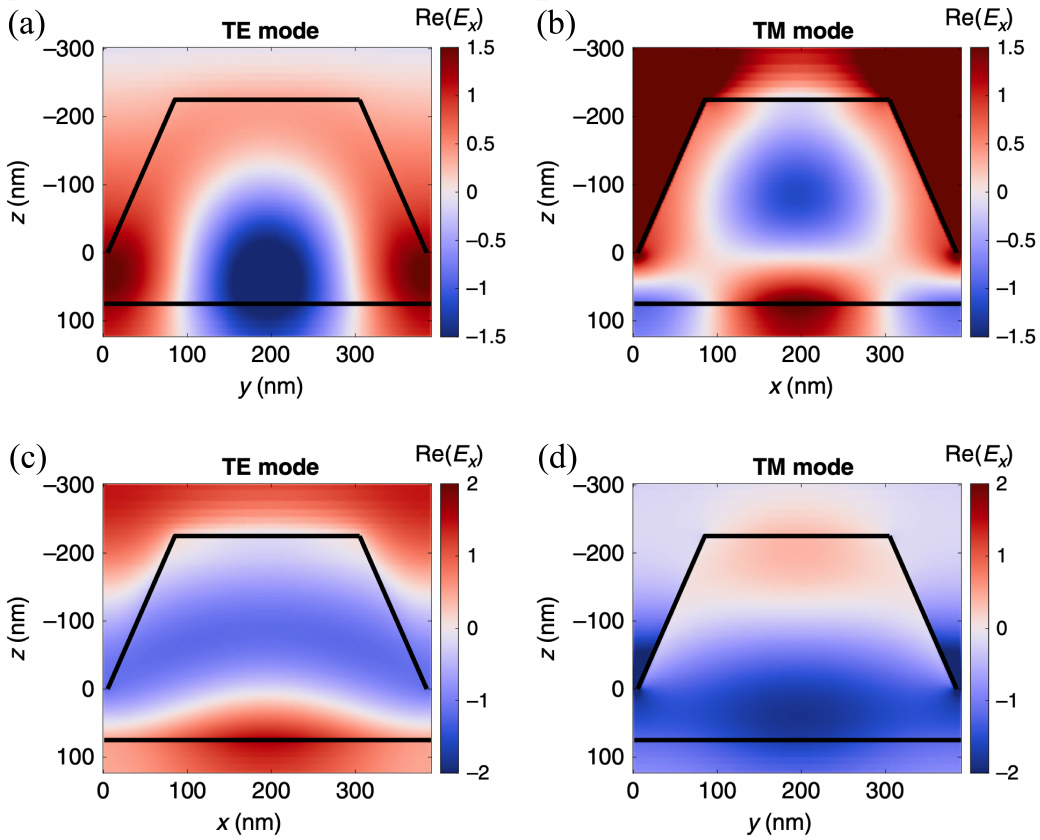

Figure 8. Real part of the electric field component E_x associated with the resonant electromagnetic field distributions for the (**a**,**c**) $TE_{0,1}$ (propagating along the *y*-axis) and (**b**,**d**) $TM_{1,0}$ (propagating along the *x*-axis) modes. Numerical results, shown inside one period of the metasurface (the cross-sections are taken at the center of the nanopillar), were calculated for a TM incident wave under normal incidence. Adapted with permission from ref. [33]. Copyright 2020 Springer Nature.

4. A Timeline View of Magneto-Optics and Its Applications

So far, we have discussed MO from their discovery up to the fusion with nanotechnology for advanced applications. Before providing our perspective on integrated magneto-photonics and its future potential industrial applications, we want to make a timeline of MO effects. Figure 9 illustrates the successive developments that have had strong influence

on the development of MO-based technology. In particular, the field of MO was relatively dormant until the mid-20th century, when novel light sources and laser technology became available [126,127]. Then, the advent of nanotechnology and modern simulation methods prompted the study of MO effects at micro- and nano-scale [128–131]. Indeed, merging femtosecond lasers with nanostructured surfaces has been recently used for ultrafast all-optical modulation of MO effects [132–134]. These current advances have made possible the emergence of time-resolved magneto-optical spectroscopy, which, in turn, allows the investigation of phenomena such as the spin relaxation of non-equilibrium photo-excited carriers, transient modifications of the ferromagnetic order, and the photo-induced dynamics phase transitions, to name just a few. In addition, the strongly enhanced MO effects in nanodevices (induced by light–matter interaction at the nanoscale) are revolutionizing several fields, including medicine [135,136], radiative energy transfer [137–139], and electronics [140,141]. On the other hand, recent studies are opening new possibilities to further understand magnetic and MO effects and their interaction with other physical quantities. For example, there are works demonstrating magnetization switching through the use of elastic strain pulses [142]. Furthermore, new microscopical theories to explain MO phenomena, based on the quantization of topological MO effects in antiferromagnetic materials [143], are promising to replace the conventional microscopic theory. Moreover, the development of new sensitivity metrics has made it possible for users to compare the performance of different kinds of sensors in a manner that is direct and independent of the biomolecular interaction between the sensors [144].

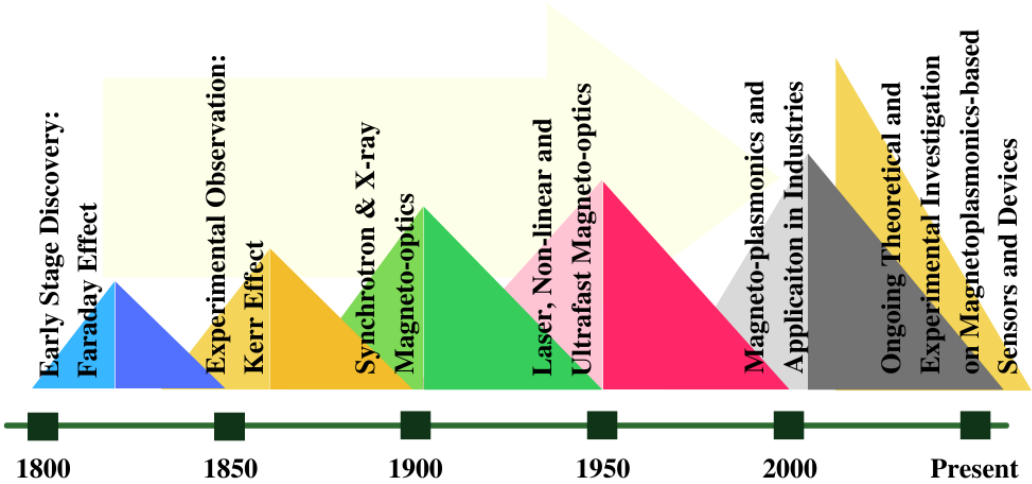

Figure 9. The origin of magneto-optics and emerging trends. 1800–1850: Early-Stage Discovery [1,145,146]: Faraday Effect; 1850–1900: Experimental Observation of the Kerr Effect [147]; 1900–1950: Synchrotron & X-ray Magneto-Optics [148]; 1950–2000: Laser, Non-linear and Ultra-fast Magneto-Optics [149]; and 2000–Present: Magnetoplasmonics [15,53,74,129,150,151], all-dielectric magnetophotonics [24,25,32,33,35,42,124], and industrial Applications [70].

5. Concluding Remarks and Outlook

New MO materials and spectroscopy methods, with significant progress for on-chip integrability with reduced optical losses have been introduced during the last several years. In particular, amplified field amplitudes in plasmonic and all-dielectric magnetophotonic nanostructures have been exploited to improve sensing performance (higher sensitivity and resolution, with enhanced limits of detection), MO modulation of optical signals (in integrated optoelectronic circuits), and magnetic control of nanoparticle trapping, among other things. MO effects are now being used for the active modulation of optical chirality in structures ranging from nanoparticle arranges to chiral metasurfaces, which may open avenues for new, efficient, cheap, and all-optical enantioseparation of drugs in the pharmaceutical industry [70]. A range of potential applications that we identified are illustrated in Figure 10. Significantly, coupling together magnetic and plasmonic properties could

provide new routes for the separation of specific biological moieties, drug delivery, and photo/magnetothermal therapies. In fact, magnetoplasmonic nanotools that act as biosensors as well as theranostic agents have already been demonstrated [152], merging SERS (surface enhanced Raman scattering) with magnetic separation, but further investigations are necessary to integrate magnetoplasmonics with microfluidics technology [153] to bring these achievements from specialized laboratories to real-life applications.

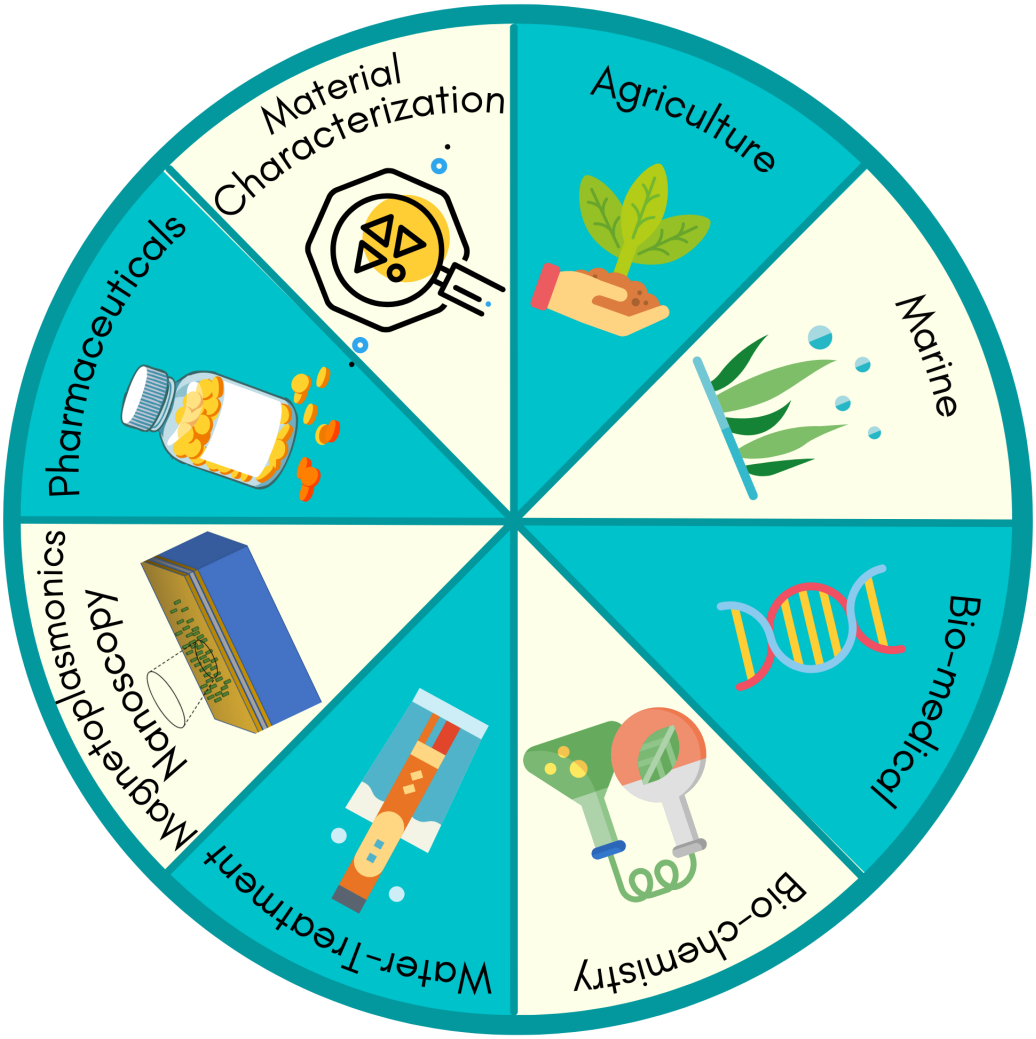

Figure 10. Potential applications of MO-SPR sensors in industry (e.g., nanostructure characterization, and label-free chemical and biological sensing) including but not limited to the following sectors: agriculture [154,155], marine [156], medical science [32,157], bio-chemistry [158], meteorology [159], nanoscopy [7–10,160], and pharmacy [70,106,161,162].

Author Contributions: Writing—original draft preparation, C.R., H.S. and J.R.M.-S.; writing—review and editing, J.R.M.-S. All authors have read and agreed to the published version of the manuscript.

Funding: H.S. acknowledges financial support from JSPS KAKENHI (Grant Number JP18K18851, JP20K20996), JST A-STEP (Grant Number JPMJTM20D1), The Murata Science Foundation, and The Casio Foundation, Japan. J.R.M.-S. acknowledges financial support from the Brazilian Agencies National Council for Scientific and Technological Development-CNPq (314671/2021-8) and RNP, with resources from MCTIC, Grant No. 01245.010604/2020-14, under the Brazil 6G project of the Radiocommunication Reference Center (Centro de Referência em Radiocomunicações—CRR) of the National Institute of Telecommunications (Instituto Nacional de Telecomunicações—Inatel), Brazil. C.R. appreciates the wage supplement provided by Biotalent Canada.

Institutional Review Board Statement: Not applicable.

Informed Consent Statement: Not applicable.

Data Availability Statement: Not applicable.

Acknowledgments: The first author would like to thank Navashikha Kandel (Georgian College, Ontario, Canada) for helping with the research and making of Figure 9.

Conflicts of Interest: The authors declare no conflict of interest. The funders had no role in the design of the study; in the collection, analyses, or interpretation of data; in the writing of the manuscript; or in the decision to publish the results.

References

1. Faraday, M. I. Experimental researches in electricity—Nineteenth series. *Philos. Trans. R. Soc. Lond.* **1846**, *136*, 1–20. [CrossRef]
2. Kerr, J. XLIII. On rotation of the plane of polarization by reflection from the pole of a magnet. *Lond. Edinb. Dublin Philos. Mag. J. Sci.* **1877**, *3*, 321–343. [CrossRef]
3. Kerr, J. XXIV. On reflection of polarized light from the equatorial surface of a magnet. *Lond. Edinb. Dublin Philos. Mag. J. Sci.* **1878**, *5*, 161–177. [CrossRef]
4. De Hoop, A.T. A reciprocity theorem for the electromagnetic field scattered by an obstacle. *Appl. Sci. Res. Sect. B* **1960**, *8*, 135–140. [CrossRef]
5. Shoji, Y.; Mizumoto, T.; Yokoi, H.; Hsieh, I.W.; Osgood, R.M. Magneto-optical isolator with silicon waveguides fabricated by direct bonding. *Appl. Phys. Lett.* **2008**, *92*, 071117. [CrossRef]
6. Srinivasan, K.; Stadler, B.J.H. Magneto-optical materials and designs for integrated TE- and TM-mode planar waveguide isolators: A review. *Opt. Mater. Express* **2018**, *8*, 3307–3318. [CrossRef]
7. Allwood, D.A.; Xiong, G.; Cooke, M.D.; Cowburn, R.P. Magneto-optical Kerr effect analysis of magnetic nanostructures. *J. Phys. D Appl. Phys.* **2003**, *36*, 2175–2182. [CrossRef]
8. Kirilyuk, A.; Kimel, A.V.; Rasing, T. Ultrafast optical manipulation of magnetic order. *RMP* **2010**, *82*, 2731–2784. [CrossRef]
9. McCord, J. Progress in magnetic domain observation by advanced magneto-optical microscopy. *J. Phys. D Appl. Phys.* **2015**, *48*, 333001. [CrossRef]
10. Higo, T.; Man, H.; Gopman, D.B.; Wu, L.; Koretsune, T.; van't Erve, O.M.J.; Kabanov, Y.P.; Rees, D.; Li, Y.; Suzuki, M.T.; et al. Large magneto-optical Kerr effect and imaging of magnetic octupole domains in an antiferromagnetic metal. *Nat. Photonics* **2018**, *12*, 73–78. [CrossRef]
11. Tufte, O.N.; Chen, D. Optical techniques for data storage. *IEEE Spectr.* **1973**, *10*, 26–32. [CrossRef]
12. Chen, D.; Zook, J.D. An overview of optical data storage technology. *Proc. IEEE* **1975**, *63*, 1207–1230. [CrossRef]
13. Mansuripur, M. *The Physical Principles of Magneto-Optical Recording*; Cambridge University Press: Cambridge, UK, 1995. [CrossRef]
14. Qin, J.; Xia, S.; Yang, W.; Wang, H.; Yan, W.; Yang, Y.; Wei, Z.; Liu, W.; Luo, Y.; Deng, L.; et al. Nanophotonic devices based on magneto-optical materials: Recent developments and applications. *Nanophotonics* **2022**, *11*, 2639–2659. [CrossRef]
15. Armelles, G.; Cebollada, A.; García-Martín, A.; González, M.U. Magnetoplasmonics: Combining magnetic and plasmonic functionalities. *Adv. Opt. Mater.* **2013**, *1*, 10–35. [CrossRef]
16. Sepúlveda, B.; González-Díaz, J.B.; García-Martín, A.; Lechuga, L.M.; Armelles, G. Plasmon-Induced Magneto-Optical Activity in Nanosized Gold Disks. *Phys. Rev. Lett.* **2010**, *104*, 147401. [CrossRef]
17. Du, G.X.; Mori, T.; Saito, S.; Takahashi, M. Shape-enhanced magneto-optical activity: Degree of freedom for active plasmonics. *Phys. Rev. B* **2010**, *82*, 161403. [CrossRef]
18. Brongersma Mark, L.; Shalaev Vladimir, M. The Case for Plasmonics. *Science* **2010**, *328*, 440–441. [CrossRef]
19. Schuller, J.A.; Barnard, E.S.; Cai, W.; Jun, Y.C.; White, J.S.; Brongersma, M.L. Plasmonics for extreme light concentration and manipulation. *Nat. Mater.* **2010**, *9*, 193–204. [CrossRef]
20. Chen, J.; Albella, P.; Pirzadeh, Z.; Alonso-González, P.; Huth, F.; Bonetti, S.; Bonanni, V.; Åkerman, J.; Nogués, J.; Vavassori, P.; et al. Plasmonic Nickel Nanoantennas. *Small* **2011**, *7*, 2341–2347. [CrossRef]
21. Maccaferri, N.; Berger, A.; Bonetti, S.; Bonanni, V.; Kataja, M.; Qin, Q.H.; van Dijken, S.; Pirzadeh, Z.; Dmitriev, A.; Nogués, J.; et al. Tuning the Magneto-Optical Response of Nanosize Ferromagnetic Ni Disks Using the Phase of Localized Plasmons. *Phys. Rev. Lett.* **2013**, *111*, 167401. [CrossRef]
22. Kataja, M.; Hakala, T.K.; Julku, A.; Huttunen, M.J.; van Dijken, S.; Törmä, P. Surface lattice resonances and magneto-optical response in magnetic nanoparticle arrays. *Nat. Commun.* **2015**, *6*, 7072. [CrossRef]
23. Temnov, V.V.; Armelles, G.; Woggon, U.; Guzatov, D.; Cebollada, A.; Garcia-Martin, A.; Garcia-Martin, J.M.; Thomay, T.; Leitenstorfer, A.; Bratschitsch, R. Active magneto-plasmonics in hybrid metal-ferromagnet structures. *Nat. Photonics* **2010**, *4*, 107–111. [CrossRef]
24. Belotelov, V.I.; Akimov, I.A.; Pohl, M.; Kotov, V.A.; Kasture, S.; Vengurlekar, A.S.; Gopal, A.V.; Yakovlev, D.R.; Zvezdin, A.K.; Bayer, M. Enhanced magneto-optical effects in magnetoplasmonic crystals. *Nat. Nanotechnol.* **2011**, *6*, 370–376. [CrossRef]
25. Kreilkamp, L.E.; Belotelov, V.I.; Chin, J.Y.; Neutzner, S.; Dregely, D.; Wehlus, T.; Akimov, I.A.; Bayer, M.; Stritzker, B.; Giessen, H. Waveguide-Plasmon Polaritons Enhance Transverse Magneto-Optical Kerr Effect. *Phys. Rev. X* **2013**, *3*, 041019. [CrossRef]

26. Sepúlveda, B.; Calle, A.; Lechuga, L.M.; Armelles, G. Highly sensitive detection of biomolecules with the magneto-optic surface-plasmon-resonance sensor. *Opt. Lett.* **2006**, *31*, 1085–1087. [CrossRef]
27. Regatos, D.; Sepúlveda, B.; Fariña, D.; Carrascosa, L.G.; Lechuga, L.M. Suitable combination of noble/ferromagnetic metal multilayers for enhanced magneto-plasmonic biosensing. *Opt. Express* **2011**, *19*, 8336–8346. [CrossRef]
28. Manera, M.G.; Ferreiro-Vila, E.; García-Martín, J.M.; Cebollada, A.; García-Martín, A.; Giancane, G.; Valli, L.; Rella, R. Enhanced magneto-optical SPR platform for amine sensing based on Zn porphyrin dimers. *Sens. Actuators B Chem.* **2013**, *182*, 232–238. [CrossRef]
29. Maccaferri, N.; Gregorczyk, K.E.; de Oliveira, T.V.A.G.; Kataja, M.; van Dijken, S.; Pirzadeh, Z.; Dmitriev, A.; Åkerman, J.; Knez, M.; Vavassori, P. Ultrasensitive and label-free molecular-level detection enabled by light phase control in magnetoplasmonic nanoantennas. *Nat. Commun.* **2015**, *6*, 6150. [CrossRef]
30. Firby, C.J.; Elezzabi, A.Y. High-speed nonreciprocal magnetoplasmonic waveguide phase shifter. *Optica* **2015**, *2*, 598–606. [CrossRef]
31. Qin, J.; Deng, L.; Kang, T.; Nie, L.; Feng, H.; Wang, H.; Yang, R.; Liang, X.; Tang, T.; Shen, J.; et al. Switching the Optical Chirality in Magnetoplasmonic Metasurfaces Using Applied Magnetic Fields. *ACS Nano* **2020**, *14*, 2808–2816. [CrossRef]
32. Voronov, A.A.; Karki, D.; Ignatyeva, D.O.; Kozhaev, M.A.; Levy, M.; Belotelov, V.I. Magneto-optics of subwavelength all-dielectric gratings. *Opt. Express* **2020**, *28*, 17988–17996. [CrossRef] [PubMed]
33. Ignatyeva, D.O.; Karki, D.; Voronov, A.A.; Kozhaev, M.A.; Krichevsky, D.M.; Chernov, A.I.; Levy, M.; Belotelov, V.I. All-dielectric magnetic metasurface for advanced light control in dual polarizations combined with high-Q resonances. *Nat. Commun.* **2020**, *11*, 5487. [CrossRef] [PubMed]
34. Carvalho, W.O.F.; Moncada-Villa, E.; Oliveira, O.N.; Mejía-Salazar, J.R. Beyond plasmonic enhancement of the transverse magneto-optical Kerr effect with low-loss high-refractive-index nanostructures. *Phys. Rev. B* **2021**, *103*, 075412. [CrossRef]
35. Carvalho, W.O.F.; Mejía-Salazar, J.R. All-dielectric magnetophotonic gratings for maximum TMOKE enhancement. *Phys. Chem. Chem. Phys.* **2022**, *24*, 5431–5436. [CrossRef]
36. Fakhrul, T.; Tazlaru, S.; Beran, L.; Zhang, Y.; Veis, M.; Ross, C.A. Magneto-Optical Bi:YIG Films with High Figure of Merit for Nonreciprocal Photonics. *Adv. Opt. Mater.* **2019**, *7*, 1900056. [CrossRef]
37. Fakhrul, T.; Tazlaru, S.; Khurana, B.; Beran, L.; Bauer, J.; Vančík, M.; Marchese, A.; Tsotsos, E.; Kučera, M.; Zhang, Y.; et al. High Figure of Merit Magneto-Optical Ce- and Bi-Substituted Terbium Iron Garnet Films Integrated on Si. *Adv. Opt. Mater.* **2021**, *9*, 2100512. [CrossRef]
38. Mizumoto, T.; Baets, R.; Bowers, J.E. Optical nonreciprocal devices for silicon photonics using wafer-bonded magneto-optical garnet materials. *MRS Bull.* **2018**, *43*, 419–424. [CrossRef]
39. Pintus, P.; Huang, D.; Morton, P.A.; Shoji, Y.; Mizumoto, T.; Bowers, J.E. Broadband TE Optical Isolators and Circulators in Silicon Photonics Through Ce:YIG Bonding. *J. Light. Technol.* **2019**, *37*, 1463–1473. [CrossRef]
40. Zhang, Y.; Du, Q.; Wang, C.; Fakhrul, T.; Liu, S.; Deng, L.; Huang, D.; Pintus, P.; Bowers, J.; Ross, C.A.; et al. Monolithic integration of broadband optical isolators for polarization-diverse silicon photonics. *Optica* **2019**, *6*, 473–478. [CrossRef]
41. Murai, T.; Shoji, Y.; Nishiyama, N.; Mizumoto, T. Nonvolatile magneto-optical switches integrated with a magnet stripe array. *Opt. Express* **2020**, *28*, 31675–31685. [CrossRef]
42. Carvalho, W.O.F.; Mejía-Salazar, J.R. Magneto-optical micro-ring resonators for dynamic tuning of add/drop channels in dense wavelength division multiplexing applications. *Opt. Lett.* **2021**, *46*, 2396–2399. [CrossRef] [PubMed]
43. Liu, S.; Shoji, Y.; Mizumoto, T. TE-mode magneto-optical isolator based on an asymmetric microring resonator under a unidirectional magnetic field. *Opt. Express* **2022**, *30*, 9934–9943. [CrossRef] [PubMed]
44. Kolmychek, I.A.; Pomozov, A.R.; Leontiev, A.P.; Napolskii, K.S.; Murzina, T.V. Magneto-optical effects in hyperbolic metamaterials. *Opt. Lett.* **2018**, *43*, 3917–3920. CrossRef] [PubMed]
45. Fan, B.; Nasir, M.E.; Nicholls, L.H.; Zayats, A.V.; Podolskiy, V.A. Magneto-Optical Metamaterials: Nonreciprocal Transmission and Faraday Effect Enhancement. *Adv. Opt. Mater.* **2019**, *7*, 1801420. [CrossRef]
46. Wang, X.; Wang, H.; Jian, J.; Rutherford, B.X.; Gao, X.; Xu, X.; Zhang, X.; Wang, H. Metal-Free Oxide-Nitride Heterostructure as a Tunable Hyperbolic Metamaterial Platform. *Nano Lett.* **2020**, *20*, 6614–6622. [CrossRef]
47. Moncada-Villa, E.; Oliveira, O.N.; Mejía-Salazar, J.R. Uniaxial ε-near-zero metamaterials for giant enhancement of the transverse magneto-optical Kerr effect. *Phys. Rev. B* **2020**, *102*, 165304. [CrossRef]
48. Wang, X.; Jian, J.; Wang, H.; Liu, J.; Pachaury, Y.; Lu, P.; Rutherford, B.X.; Gao, X.; Xu, X.; El-Azab, A.; et al. Nitride-Oxide-Metal Heterostructure with Self-Assembled Core-Shell Nanopillar Arrays: Effect of Ordering on Magneto-Optical Properties. *Small* **2021**, *17*, 2007222. [CrossRef]
49. Pershan, P.S. Magneto-Optical Effects. *J. Appl. Phys.* **1967**, *38*, 1482–1490. [CrossRef]
50. Chen, D. Magneto-Optic Principles, Materials And Applications. In Proceedings of the Electro-Optics Principles and Applications, Boston, MA, USA, 1–2 January 1973; Volume 0038. [CrossRef]
51. Mansuripur, M. The Faraday Effect. *Opt. Photon. News* **1999**, *10*, 32–36. [CrossRef]
52. Qiu, Z.Q.; Bader, S.D. Surface magneto-optic Kerr effect. *Rev. Sci. Instrum.* **2000**, *71*, 1243–1255. [CrossRef]
53. Floess, D.; Giessen, H. Nonreciprocal hybrid magnetoplasmonics. *Rep. Prog. Phys.* **2018**, *81*, 116401. [CrossRef] [PubMed]
54. Maccaferri, N.; Zubritskaya, I.; Razdolski, I.; Chioar, I.A.; Belotelov, V.; Kapaklis, V.; Oppeneer, P.M.; Dmitriev, A. Nanoscale magnetophotonics. *J. Appl. Phys.* **2020**, *127*, 080903. [CrossRef]

55. Wood, R.W. XLII. On a remarkable case of uneven distribution of light in a diffraction grating spectrum. *Lond. Edinb. Dublin Philos. Mag. J. Sci.* **1902**, *4*, 396–402. [CrossRef]
56. Rayleigh, L. III. Note on the remarkable case of diffraction spectra described by Prof. Wood. *Lond. Edinb. Dublin Philos. Mag. J. Sci.* **1907**, *14*, 60–65. [CrossRef]
57. Rayleigh, L. On the dynamical theory of gratings. *Proc. R. Soc. Lond. Ser. A Contain. Pap. Math. Phys. Character* **1907**, *79*, 399–416. [CrossRef]
58. Fano, U. The Theory of Anomalous Diffraction Gratings and of Quasi-Stationary Waves on Metallic Surfaces (Sommerfeld's Waves). *J. Opt. Soc. Am.* **1941**, *31*, 213–222. [CrossRef]
59. Bohm, D.; Pines, D. A Collective Description of Electron Interactions. I. Magnetic Interactions. *Phys. Rev.* **1951**, *82*, 625–634. [CrossRef]
60. Pines, D.; Bohm, D. A Collective Description of Electron Interactions: II. Collective vs Individual Particle Aspects of the Interactions. *Phys. Rev.* **1952**, *85*, 338–353. [CrossRef]
61. Pines, D. A Collective Description of Electron Interactions: IV. Electron Interaction in Metals. *Phys. Rev.* **1953**, *92*, 626–636. [CrossRef]
62. Bohm, D.; Pines, D. A Collective Description of Electron Interactions: III. Coulomb Interactions in a Degenerate Electron Gas. *Phys. Rev.* **1953**, *92*, 609–625. [CrossRef]
63. Ritchie, R.H. Plasma Losses by Fast Electrons in Thin Films. *Phys. Rev.* **1957**, *106*, 874–881. [CrossRef]
64. Powell, C.J.; Swan, J.B. Origin of the Characteristic Electron Energy Losses in Aluminum. *Phys. Rev.* **1959**, *115*, 869–875. [CrossRef]
65. Kretschmann, E.; Raether, H. Notizen: Radiative Decay of Non Radiative Surface Plasmons Excited by Light. *Z. Für Naturforschung A* **1968**, *23*, 2135–2136. [CrossRef]
66. Otto, A. Excitation of nonradiative surface plasma waves in silver by the method of frustrated total reflection. *Z. Für Phys. A Hadron. Nucl.* **1968**, *216*, 398–410. [CrossRef]
67. Stockman, M.I. Nanoplasmonics: Past, present, and glimpse into future. *Opt. Express* **2011**, *19*, 22029–22106. [CrossRef]
68. Maxwell-Garnett, J.C. XII. Colours in metal glasses and in metallic films. *Philos. Trans. R. Soc. Lond. Ser. A Contain. Pap. Math. Phys. Character* **1904**, *203*, 385–420. [CrossRef]
69. Mie, G. Beiträge zur Optik trüber Medien, speziell kolloidaler Metallösungen. *Ann. Phys.* **1908**, *330*, 377–445. [CrossRef]
70. Rizal, C.; Manera, M.G.; Ignatyeva, D.O.; Mejía-Salazar, J.R.; Rella, R.; Belotelov, V.I.; Pineider, F.; Maccaferri, N. Magnetophotonics for sensing and magnetometry toward industrial applications. *J. Appl. Phys.* **2021**, *130*, 230901. [CrossRef]
71. Nylander, C.; Liedberg, B.; Lind, T. Gas detection by means of surface plasmon resonance. *Sens. Actuators* **1982**, *3*, 79–88. [CrossRef]
72. Liedberg, B.; Nylander, C.; Lunström, I. Surface plasmon resonance for gas detection and biosensing. *Sens. Actuators* **1983**, *4*, 299–304. [CrossRef]
73. Mejía-Salazar, J.R.; Oliveira, O.N. Plasmonic Biosensing. *Chem. Rev.* **2018**, *118*, 10617–10625. [CrossRef] [PubMed]
74. Guo, J.; Zhu, Z.; Deng, W. Small-angle measurement based on surface-plasmon resonance and the use of magneto-optical modulation. *Appl. Opt.* **1999**, *38*, 6550–6555. [CrossRef] [PubMed]
75. David, S.; Polonschii, C.; Luculescu, C.; Gheorghiu, M.; Gáspár, S.; Gheorghiu, E. Magneto-plasmonic biosensor with enhanced analytical response and stability. *Biosens. Bioelectron.* **2015**, *63*, 525–532. [CrossRef]
76. Diaz-Valencia, B.F.; Mejía-Salazar, J.R.; Oliveira, O.N.; Porras-Montenegro, N.; Albella, P. Enhanced Transverse Magneto-Optical Kerr Effect in Magnetoplasmonic Crystals for the Design of Highly Sensitive Plasmonic (Bio)sensing Platforms. *ACS Omega* **2017**, *2*, 7682–7685. [CrossRef]
77. Tran, V.T.; Kim, J.; Tufa, L.T.; Oh, S.; Kwon, J.; Lee, J. Magnetoplasmonic Nanomaterials for Biosensing/Imaging and in Vitro/in Vivo Biousability. *Anal. Chem.* **2018**, *90*, 225–239. [CrossRef] [PubMed]
78. Abujetas, D.R.; de Sousa, N.; García-Martín, A.; Llorens, J.M.; Sánchez-Gil, J.A. Active angular tuning and switching of Brewster quasi bound states in the continuum in magneto-optic metasurfaces. *Nanophotonics* **2021**, *10*, 4223–4232. [CrossRef]
79. Kausaite-Minkstimiene, A.; Popov, A.; Ramanaviciene, A. Surface Plasmon Resonance Immunosensor with Antibody-Functionalized Magnetoplasmonic Nanoparticles for Ultrasensitive Quantification of the CD5 Biomarker. *ACS Appl. Mater. Interfaces* **2022**, *14*, 20720–20728. [CrossRef]
80. Tsakmakidis, K. Non-reciprocal plasmonics. *Nat. Mater.* **2013**, *12*, 378. [CrossRef]
81. Shastri, K.; Abdelrahman, M.I.; Monticone, F. Nonreciprocal and Topological Plasmonics. *Photonics* **2021**, *8*, 133. [CrossRef]
82. Wang, J.; Shi, Q.Y.; Liu, Y.J.; Dong, H.Y.; Fung, K.H.; Dong, Z.G. Stopping surface magneto-plasmons by non-reciprocal graded waveguides. *Phys. Lett. A* **2021**, *398*, 127279. [CrossRef]
83. Shimizu, H.; Zayets, V. Plasmonic isolator for photonic integrated circuits. *MRS Bull.* **2018**, *43*, 425–429. [CrossRef]
84. Armelles, G.; Caballero, B.; Prieto, P.; García, F.; Cebollada, A.; González, M.U.; García-Martin, A. Magnetic field modulation of chirooptical effects in magnetoplasmonic structures. *Nanoscale* **2014**, *6*, 3737–3741. [CrossRef] [PubMed]
85. Yannopapas, V. Magnetochirality in hierarchical magnetoplasmonic clusters. *Solid State Commun.* **2015**, *217*, 47–52. [CrossRef]
86. Feng, H.Y.; de Dios, C.; García, F.; Cebollada, A.; Armelles, G. Analysis and magnetic modulation of chiro-optical properties in anisotropic chiral and magneto-chiral plasmonic systems. *Opt. Express* **2017**, *25*, 31045–31055. [CrossRef]
87. Wu, X.; Hao, C.; Xu, L.; Kuang, H.; Xu, C. Chiromagnetic Plasmonic Nanoassemblies with Magnetic Field Modulated Chiral Activity. *Small* **2020**, *16*, 1905734. [CrossRef]

88. Wang, N.; Ding, L.; Wang, W. Magnetoplasmonic coupling in graphene nanodisk dimers: An extended coupled-dipole model for circularly polarized states. *Phys. Rev. B* **2022**, *105*, 235435. [CrossRef]
89. Nguyen, H.Q.; Hwang, D.; Park, S.; Nguyen, M.C.T.; Kang, S.S.; Tran, V.T.; Lee, J. One-Pot Synthesis of Magnetoplasmonic Au@FexOy Nanowires: Bioinspired Bouligand Chiral Stack. *ACS Nano* **2022**, *16*, 5795–5806. [CrossRef]
90. Baron Kelvin, W.T. *Baltimore Lectures on Molecular Dynamics and the Wave Theory of Light*; Cambridge University Press: Cambridge, UK, 2010. [CrossRef]
91. Barron, L. Chirality and Life. In *Strategies of Life Detection*; Botta, O., Bada, J.L., Gomez-Elvira, J., Javaux, E., Selsis, F., Summons, R., Eds.; Springer: Boston, MA, USA, 2008; pp. 187–201. [CrossRef]
92. Inaki, M.; Liu, J.; Matsuno, K. Cell chirality: Its origin and roles in left-right asymmetric development. *Philos. Trans. R. Soc. B Biol. Sci.* **2016**, *371*, 20150403. [CrossRef]
93. McConathy, J.; Owens, M.J. Stereochemistry in Drug Action. *Prim. Care Companion J. Clin. Psychiatry* **2003**, *5*, 70–73. [CrossRef]
94. Singh, K.; Shakya, P.; Kumar, A.H.S.; Alok, S.; Kamal, M.; Singh, S.P. Stereochemistry and its role in drug design. *Int. J. Pharm. Sci. Res.* **2014**, *5*, 4644–4659.
95. Du, X.; Zhou, J.; Wang, J.; Zhou, R.; Xu, B. Chirality Controls Reaction-Diffusion of Nanoparticles for Inhibiting Cancer Cells. *ChemNanoMat* **2017**, *3*, 17–21. [CrossRef] [PubMed]
96. Nguyen, L.A.; He, H.; Pham-Huy, C. Chiral drugs: An overview. *Int. J. Biomed. Sci. IJBS* **2006**, *2*, 85–100. [PubMed]
97. Smith, S.W. Chiral Toxicology: It's the Same Thing…Only Different. *Toxicol. Sci.* **2009**, *110*, 4–30. [CrossRef] [PubMed]
98. Tokunaga, E.; Yamamoto, T.; Ito, E.; Shibata, N. Understanding the Thalidomide Chirality in Biological Processes by the Self-disproportionation of Enantiomers. *Sci. Rep.* **2018**, *8*, 17131. [CrossRef]
99. Rodger, A. Circular Dichroism and Linear Dichroism. In *Encyclopedia of Analytical Chemistry*; John Wiley & Sons, Ltd.: Hoboken, NJ, USA, 2014; pp. 1–34. [CrossRef]
100. Liu, Z.; Du, Y.; Feng, Z. Enantioseparation of drugs by capillary electrochromatography using a stationary phase covalently modified with graphene oxide. *Microchim. Acta* **2017**, *184*, 583–593. [CrossRef]
101. Gwak, J.; Park, S.J.; Choi, H.Y.; Lee, J.H.; Jeong, K.J.; Lee, D.; Tran, V.T.; Son, K.S.; Lee, J. Plasmonic Enhancement of Chiroptical Property in Enantiomers Using a Helical Array of Magnetoplasmonic Nanoparticles for Ultrasensitive Chiral Recognition. *ACS Appl. Mater. Interfaces* **2021**, *13*, 46886–46893. [CrossRef]
102. Atzori, M.; Rikken, G.L.J.A.; Train, C. Magneto-Chiral Dichroism: A Playground for Molecular Chemists. *Chem. Eur. J.* **2020**, *26*, 9784–9791. [CrossRef]
103. Petrucci, G.; Gabbani, A.; Faniayeu, I.; Pedrueza-Villalmanzo, E.; Cucinotta, G.; Atzori, M.; Dmitriev, A.; Pineider, F. Macroscopic magneto-chiroptical metasurfaces. *Appl. Phys. Lett.* **2021**, *118*, 251108. [CrossRef]
104. Li, C.; Li, S.; Zhao, J.; Sun, M.; Wang, W.; Lu, M.; Qu, A.; Hao, C.; Chen, C.; Xu, C.; et al. Ultrasmall Magneto-chiral Cobalt Hydroxide Nanoparticles Enable Dynamic Detection of Reactive Oxygen Species in Vivo. *J. Am. Chem. Soc.* **2022**, *144*, 1580–1588. [CrossRef]
105. Zubritskaya, I.; Maccaferri, N.; Inchausti Ezeiza, X.; Vavassori, P.; Dmitriev, A. Magnetic Control of the Chiroptical Plasmonic Surfaces. *Nano Lett.* **2018**, *18*, 302–307. [CrossRef]
106. Girón-Sedas, J.A.; Mejía-Salazar, J.R.; Granada, J.C.; Oliveira, O.N. Repulsion of polarized particles near a magneto-optical metamaterial. *Phys. Rev. B* **2016**, *94*, 245430. [CrossRef]
107. Maccaferri, N.; Vavassori, P.; Garoli, D. Magnetic control of particle trapping in a hybrid plasmonic nanopore. *Appl. Phys. Lett.* **2021**, *118*, 193102. [CrossRef]
108. Biagioni, P.; Huang, J.S.; Hecht, B. Nanoantennas for visible and infrared radiation. *Rep. Prog. Phys.* **2012**, *75*, 024402. [CrossRef] [PubMed]
109. Boriskina, S.V.; Cooper, T.A.; Zeng, L.; Ni, G.; Tong, J.K.; Tsurimaki, Y.; Huang, Y.; Meroueh, L.; Mahan, G.; Chen, G. Losses in plasmonics: From mitigating energy dissipation to embracing loss-enabled functionalities. *Adv. Opt. Photonics* **2017**, *9*, 775–827. [CrossRef]
110. Hernández-Sarria, J.J.; Oliveira, O.N.; Mejía-Salazar, J.R. Toward Lossless Infrared Optical Trapping of Small Nanoparticles Using Nonradiative Anapole Modes. *Phys. Rev. Lett.* **2021**, *127*, 186803. [CrossRef]
111. Decker, M.; Staude, I. Resonant dielectric nanostructures: A low-loss platform for functional nanophotonics. *J. Opt.* **2016**, *18*, 103001. [CrossRef]
112. Kuznetsov Arseniy, I.; Miroshnichenko Andrey, E.; Brongersma Mark, L.; Kivshar Yuri, S.; Boris, L. Optically resonant dielectric nanostructures. *Science* **2016**, *354*, aag2472. [CrossRef]
113. Huang, T.; Wang, B.; Zhang, W.; Zhao, C. Ultracompact Energy Transfer in Anapole-based Metachains. *Nano Lett.* **2021**, *21*, 6102–6110. [CrossRef]
114. Bi, L.; Hu, J.; Jiang, P.; Kim, H.S.; Kim, D.H.; Onbasli, M.C.; Dionne, G.F.; Ross, C.A. Magneto-Optical Thin Films for On-Chip Monolithic Integration of Non-Reciprocal Photonic Devices. *Materials* **2013**, *6*, 5094–5117. [CrossRef]
115. Onbasli, M.C.; Goto, T.; Sun, X.; Huynh, N.; Ross, C.A. Integration of bulk-quality thin film magneto-optical cerium-doped yttrium iron garnet on silicon nitride photonic substrates. *Opt. Express* **2014**, *22*, 25183–25192. [CrossRef]
116. Onbasli, M.C.; Beran, L.; Zahradník, M.; Kučera, M.; Antoš, R.; Mistrík, J.; Dionne, G.F.; Veis, M.; Ross, C.A. Optical and magneto-optical behavior of Cerium Yttrium Iron Garnet thin films at wavelengths of 200–1770 nm. *Sci. Rep.* **2016**, *6*, 23640. [CrossRef] [PubMed]

117. Permin, D.A.; Novikova, A.V.; Koshkin, V.A.; Balabanov, S.S.; Snetkov, I.L.; Palashov, O.V.; Smetanina, K.E. Fabrication and Magneto-Optical Properties of Yb_2O_3 Based Ceramics. *Magnetochemistry* **2020**, *6*, 63. [CrossRef]
118. Aung, Y.L.; Ikesue, A.; Yasuhara, R.; Iwamoto, Y. Magneto-optical Dy2O3 ceramics with optical grade. *Opt. Lett.* **2020**, *45*, 4615–4617. [CrossRef]
119. Dai, J.; Li, J. Promising magneto-optical ceramics for high power Faraday isolators. *Scr. Mater.* **2018**, *155*, 78–84. [CrossRef]
120. Ikesue, A.; Aung, Y.L. Magneto-Optic Transparent Ceramics. In *Processing of Ceramics*; John Wiley & Sons, Ltd.: Hoboken, NJ, USA, 2021; Chapter 4, pp. 143–185. [CrossRef]
121. Murai, T.; shoji, Y.; Mizumoto, T. Light-induced thermomagnetic recording of thin-film magnet CoFeB on silicon waveguide for on-chip magneto-optical memory. *Opt. Express* **2022**, *30*, 18054–18065. [CrossRef]
122. Rostova, E.; Ben Adiba, C.; Dietler, G.; Sekatskii, S.K. Kinetics of Antibody Binding to Membranes of Living Bacteria Measured by a Photonic Crystal-Based Biosensor. *Biosensors* **2016**, *6*, 52. [CrossRef]
123. Borovkova, O.V.; Ignatyeva, D.O.; Sekatskii, S.K.; Karabchevsky, A.; Belotelov, V.I. High-Q surface electromagnetic wave resonance excitation in magnetophotonic crystals for supersensitive detection of weak light absorption in the near-infrared. *Photon. Res.* **2020**, *8*, 57–64. [CrossRef]
124. Chernov, A.I.; Kozhaev, M.A.; Ignatyeva, D.O.; Beginin, E.N.; Sadovnikov, A.V.; Voronov, A.A.; Karki, D.; Levy, M.; Belotelov, V.I. All-Dielectric Nanophotonics Enables Tunable Excitation of the Exchange Spin Waves. *Nano Lett.* **2020**, *20*, 5259–5266. [CrossRef]
125. Zimnyakova, P.E.; Ignatyeva, D.O.; Karki, D.; Voronov, A.A.; Shaposhnikov, A.N.; Berzhansky, V.N.; Levy, M.; Belotelov, V.I. Two-dimensional array of iron-garnet nanocylinders supporting localized and lattice modes for the broadband boosted magneto-optics. *Nanophotonics* **2022**, *11*, 119–127. [CrossRef]
126. Gerasimov, M.V.; Logunov, M.V.; Spirin, A.V.; Nozdrin, Y.N.; Tokman, I.D. Time evolution of domain-wall motion induced by nanosecond laser pulses. *Phys. Rev. B* **2016**, *94*, 014434. [CrossRef]
127. Fanciulli, M.; Bresteau, D.; Vimal, M.; Luttmann, M.; Sacchi, M.; Ruchon, T. Electromagnetic theory of helicoidal dichroism in reflection from magnetic structures. *Phys. Rev. A* **2021**, *103*, 013501. [CrossRef]
128. Berger, A.; Alcaraz de la Osa, R.; Suszka, A.K.; Pancaldi, M.; Saiz, J.M.; Moreno, F.; Oepen, H.P.; Vavassori, P. Enhanced Magneto-Optical Edge Excitation in Nanoscale Magnetic Disks. *Phys. Rev. Lett.* **2015**, *115*, 187403. [CrossRef] [PubMed]
129. Manera, M.G.; Colombelli, A.; Taurino, A.; Martin, A.G.; Rella, R. Magneto-Optical properties of noble-metal nanostructures: Functional nanomaterials for bio sensing. *Sci. Rep.* **2018**, *8*, 12640. [CrossRef] [PubMed]
130. Nedoliuk, I.O.; Hu, S.; Geim, A.K.; Kuzmenko, A.B. Colossal infrared and terahertz magneto-optical activity in a two-dimensional Dirac material. *Nat. Nanotechnol.* **2019**, *14*, 756–761. [CrossRef]
131. Zdoroveyshchev, A.V.; Vikhrova, O.V.; Demina, P.B.; Dorokhin, M.V.; Kudrin, A.V.; Temiryazev, A.G.; Temiryazeva, M.P. Magneto-Optical and Micromagnetic Properties of Ferromagnet/Heavy Metal Thin Film Structures. *Int. J. Nanosci.* **2019**, *18*, 1940019. [CrossRef]
132. Siegrist, F.; Gessner, J.A.; Ossiander, M.; Denker, C.; Chang, Y.P.; Schröder, M.C.; Guggenmos, A.; Cui, Y.; Walowski, J.; Martens, U.; et al. Light-wave dynamic control of magnetism. *Nature* **2019**, *571*, 240–244. [CrossRef]
133. Novikov, I.A.; Kiryanov, M.A.; Nurgalieva, P.K.; Frolov, A.Y.; Popov, V.V.; Dolgova, T.V.; Fedyanin, A.A. Ultrafast Magneto-Optics in Nickel Magnetoplasmonic Crystals. *Nano Lett.* **2020**, *20*, 8615–8619. [CrossRef]
134. Möller, C.; Probst, H.; Otto, J.; Stroh, K.; Mahn, C.; Steil, S.; Moshnyaga, V.; Jansen, G.S.M.; Steil, D.; Mathias, S. Ultrafast element-resolved magneto-optics using a fiber-laser-driven extreme ultraviolet light source. *Rev. Sci. Instrum.* **2021**, *92*, 065107. [CrossRef]
135. Ando, Y.; Ogawa, K.; Hashimoto, S. Clinical application of a magneto-optical disk image filing system/image save and carry (ISAC) system. *Comput. Methods Programs Biomed.* **1991**, *36*, 125–129. [CrossRef]
136. McBirney, S.; Chen, D.; Scholtz, A.; Ameri, H.; Armani, A.M. Rapid Diagnostic for Point-of-Care Malaria Screening. *ACS Sens.* **2018**, *3*, 1264–1270. [CrossRef]
137. Moncada-Villa, E.; Fernández-Hurtado, V.; García-Vidal, F.J.; García-Martín, A.; Cuevas, J.C. Magnetic field control of near-field radiative heat transfer and the realization of highly tunable hyperbolic thermal emitters. *Phys. Rev. B* **2015**, *92*, 125418. [CrossRef]
138. Moncada-Villa, E.; Cuevas, J.C. Magnetic field effects in the near-field radiative heat transfer between planar structures. *Phys. Rev. B* **2020**, *101*, 085411. [CrossRef]
139. Abrantes, P.P.; Bastos, G.; Szilard, D.; Farina, C.; Rosa, F.S.S. Tuning resonance energy transfer with magneto-optical properties of graphene. *Phys. Rev. B* **2021**, *103*, 174421. [CrossRef]
140. Zayets, V.; Ando, K. Magneto-Optical Devices for Optical Integrated Circuits. In *Frontiers in Guided Wave Optics and Optoelectronics*; Pal, B., Ed.; IntechOpen: Rijeka, Croatia, 2010; Chapter 16. [CrossRef]
141. Protopopov, V.; Protopopov, V. Magneto-Optics. In *Practical Opto-Electronics: An Illustrated Guide for the Laboratory*; Springer International Publishing: Cham, Switzerland, 2014; pp. 231–252. [CrossRef]
142. Vlasov, V.S.; Lomonosov, A.M.; Golov, A.V.; Kotov, L.N.; Besse, V.; Alekhin, A.; Kuzmin, D.A.; Bychkov, I.V.; Temnov, V.V. Magnetization switching in bistable nanomagnets by picosecond pulses of surface acoustic waves. *Phys. Rev. B* **2020**, *101*, 024425. [CrossRef]
143. Feng, W.; Hanke, J.P.; Zhou, X.; Guo, G.Y.; Blügel, S.; Mokrousov, Y.; Yao, Y. Topological magneto-optical effects and their quantization in noncoplanar antiferromagnets. *Nat. Commun.* **2020**, *11*, 118. [CrossRef]
144. Rizal, C. Magneto-Optic-Plasmonic sensors with improved performance. *IEEE Trans. Magn.* **2021**, *57*, 4000405. [CrossRef]

145. Faraday, M. V. Experimental researches in electricity. *Philos. Trans. R. Soc. Lond.* **1832**, *122*, 125–162.
146. Hare, R. LXXIV. Second letter to Prof. Faraday. *Lond. Edinb. Dublin Philos. Mag. J. Sci.* **1841**, *18*, 465–477. [CrossRef]
147. Weinberger, P. John Kerr and his effects found in 1877 and 1878. *Philos. Mag. Lett.* **2008**, *88*, 897–907. [CrossRef]
148. Starke, K.; Heigl, F.; Prieto, J.; Krupin, O.; Vollmer, A.; Reichardt, G.; Senf, F.; Follath, R.; Brookes, N.; Kaindl, G. X-ray Magneto-Optics. In *Advances in Solid State Physics*; Springer: Berlin/Heidelberg, Germany, 2001; pp. 161–170.
149. Lalieu, M.L.; Koopmans, B. Magneto-optics and Laser-Induced Dynamics of Metallic Thin Films. In *Handbook of Magnetism and Magnetic Materials*; Springer: Berlin/Heidelberg, Germany, 2021; pp. 477–547.
150. Gabbani, A.; Petrucci, G.; Pineider, F. Magneto-optical methods for magnetoplasmonics in noble metal nanostructures. *J. Appl. Phys.* **2021**, *129*, 211101. [CrossRef]
151. Rizal, C.; Belotelov, V.; Ignatyeva, D.; Zvezdin, A.K.; Pisana, S. Surface plasmon resonance (SPR) to magneto-optic SPR. *Condens. Matter* **2019**, *4*, 50. [CrossRef]
152. Del Tedesco, A.; Piotto, V.; Sponchia, G.; Hossain, K.; Litti, L.; Peddis, D.; Scarso, A.; Meneghetti, M.; Benedetti, A.; Riello, P. Zirconia-Based Magnetoplasmonic Nanocomposites: A New Nanotool for Magnetic-Guided Separations with SERS Identification. *ACS Appl. Nano Mater.* **2020**, *3*, 1232–1241. [CrossRef]
153. Mejía-Salazar, J.R.; Rodrigues Cruz, K.; Materón Vásques, E.M.; Novais de Oliveira, O., Jr. Microfluidic Point-of-Care Devices: New Trends and Future Prospects for eHealth Diagnostics. *Sensors* **2020**, *20*, 1951. [CrossRef] [PubMed]
154. Kalabina, N.A.; Ksenevich, T.I.; Beloglazov, A.A.; Nikitin, P.I. Pesticide sensing by surface-plasmon resonance. In *Optical Sensors for Environmental and Chemical Process Monitoring*; SPIE: Bellingham, WA, USA, 1995; Volume 2367, pp. 126–132.
155. Bernieri, T.; Rodrigues, D.; Barbosa, I.R.; Ardenghi, P.G.; da Silva, L.B. Occupational exposure to pesticides and thyroid function in Brazilian soybean farmers. *Chemosphere* **2019**, *218*, 425–429. [CrossRef]
156. Prado, E.; Colas, F.; Laurent, S.; Tardivel, M.; Evrard, J.; Forest, B.; Bocher, A.; Rouxel, J. Toward a SPR imaging in situ system to detect marine biotoxin. In Proceedings of the Biophotonics in Point-of-Care, Online, 6–10 April 2020; Volume 11361, pp. 15–26.
157. Pal, A.; Bisht, S.; Sharma, A.; Panwar, B.; Bhayana, D.A.; Sharma, S.; Srivastava, S. Prism based surface plasmon resonance biosensor for biomedical applications. In *ICOL-2019*; Springer: Berlin/Heidelberg, Germany, 2021; pp. 437–440.
158. Wang, W.; Thiemann, S.; Chen, Q. Utility of SPR technology in biotherapeutic development: Qualification for intended use. *Anal. Biochem.* **2022**, *654*, 114804. [CrossRef]
159. Ignatov, A.I.; Merzlikin, A.M. Two optical sensing elements for H2O and NO2 gas sensing based on the single plasmonic–photonic crystal slab. *Adv. Opt. Technol.* **2020**, *9*, 203–208. [CrossRef]
160. Abedin, S.; Kenison, J.; Vargas, C.; Potma, E.O. Sensing biomolecular interactions by the luminescence of a planar gold film. *Anal. Chem.* **2019**, *91*, 15883–15889. [CrossRef]
161. Moura, C.; André, I.; Neves, F.; Pereira, M.; Almeida, M.; Oliveira, M.; Bento, M.; Taborda, N.; Cruz, R.; Cordeiro, R.; et al. LxUs. 2021. Available online: https://www.sensus.org/team-result-documents-2021 (accessed on 15 July 2022).
162. Rizal, C. Magneto-optic SPR-based Biosensors. In Proceedings of the 2020 Photonics North (PN), Niagara Falls, ON, Canada, 26–28 May 2020; p. 1.